

# AN ATOMISTIC MODEL OF INTERMOLECULAR INTERACTIONS FOR SIMULATIONS OF LIQUID *n*-OCTANE

MODELO ATOMÍSTICO DE LAS INTERACCIONES INTERMOLECULARES PARA LA SIMULACIÓN DEL LÍQUIDO DE *n*-OCTANO

B. RODRÍGUEZ-HERNÁNDEZ, L. URANGA PIÑA<sup>†</sup>, A. MARTÍNEZ MESA

Facultad de Física, Universidad de La Habana, Cuba. llinersy@fisica.uh.cu<sup>†</sup>

<sup>†</sup> corresponding author

(Recibido 22/3/2014 ; Aceptado 22/7/2014)

**PACS:** Computer simulation of molecular dynamics, 83.10.Rs; Molecular dynamics calculations in liquid structure modeling, 61.20.Ja; Structure of molecular liquids, 61.25.Em

During the last decades, the investigation of dynamical processes at the molecular scale have being largely dominated by the application of Classical Molecular Dynamics (CMD) simulations. In physical and chemical phenomena, classical mechanics often provides an adequate description of underlying nuclear motion, which can be extended up to thousands of atoms and up to the nanosecond or microsecond time-scales [1]. However, an accurate knowledge of the relevant intermolecular interactions is a prerequisite for dynamical calculations, and *ab initio* electronic structure calculations for relatively large molecular systems continue to pose a tremendous challenge to modern computational physics. As a consequence, assessing the performance of force-fields determined in advance, regarding their ability to reproduce the structural and thermodynamic properties measured in the experiment, is one of the main goals of the molecular dynamics scheme. The united-atom scheme [2–4] leads to a major simplification of the parametrization of the potential energy surface. Within this model, large molecules are replaced by pseudo-atoms located at positions selected according to the symmetry of the molecules.

Simple organic molecules are among the systems for which the application of the united-atom strategy is more interesting, since the representations of intermolecular forces validated for these molecules are expected to be directly transferable to the simulation of the physical properties of a wide range of organic compounds [5–8]. On the other hand, the smallest hydrocarbons are key elements in biological and industrial processes. Moreover, when used as solvents in molecular spectroscopy studies, some substances like *n*-octane exhibit remarkable properties for which a satisfactory explanation is still lacking. For example, the absorption and fluorescence spectra of some molecules solved in *n*-octane, present bands whose intensities do not match each other [9]. Due to the

practical importance of these substances, it is highly desirable to count with fairly simple representations of intermolecular forces for the calculation of observables in the liquid phase, without compromising accuracy. In particular, *n*-octane has many applications in organic synthesis and distillation, and it is one of the fundamental components of gasoline and other oil derivatives.

The purpose of present work is to attain an atomistic description of intermolecular interactions in liquid *n*-octane, which will be applied to the CMD simulation of this substance. The model introduced here disregards the structure of the molecule, though it is incorporated implicitly in the interaction potential derived from this assumption. The thermodynamics properties of *n*-octane are evaluated for a wide range of thermodynamic conditions.

We will consider that the microscopic structure of liquid *n*-octane, as well as its physical properties, can be mimicked by a Lennard-Jones (LJ) fluid with suitable energy,  $\epsilon$ , and length,  $\sigma$ , parameters. The Lennard-Jones fluid is defined by the pair potential:

$$U_{LJ}(r) = 4\epsilon \left[ \left( \frac{\sigma}{r} \right)^{12} - \left( \frac{\sigma}{r} \right)^6 \right]. \quad (1)$$

Another useful model for liquids consisting in featureless particles is that of the hard sphere (HS) fluid. In this case, the interparticle interaction potential is given by

$$U_{HS}(r) = \begin{cases} \infty, & r < d \\ 0, & r \geq d \end{cases} \quad (2)$$

where  $d$  is a hard sphere diameter.

Contrary to the Lennard-Jones fluid, the thermodynamic

properties of a system of hard spheres admit analytical representation. Therefore, the HS liquid is very amenable as a starting point for the fitting of empirical data, in order to produce a simple pairwise model of interactions in n-octane. In this work, we have considered the Barker-Henderson perturbation theory [10,11], to the aim of computing the properties of a Lennard-Jones fluid from that of a reference hard sphere liquid. The properties of the HS fluid can be expressed as functions of the packing fraction

$$\eta = \frac{\pi}{6} \rho d^3, \quad (3)$$

where  $\rho$  is the average density of the liquid at a given pressure  $P$  and temperature  $T$ .

The Helmholtz free energy of the LJ system can be expressed as [12]:

$$F_{LJ} = F_{HS} + e^{-\eta^2} \rho kT \Delta B_2 + \varepsilon \sum_{i,j} C_{i,j} T^{\frac{i}{2}} (\rho \sigma^3)^j, \quad (4)$$

where  $F_{HS}$  is the Helmholtz free energy for the fluid of hard spheres, defined by

$$F_{HS} = kT \left[ \frac{5}{3} \ln(1 - \eta) + \frac{\eta(34 - 33\eta^2)}{6(1 - \eta)^2} \right]. \quad (5)$$

The quantity  $\Delta B_2$  is the residual second virial coefficient, i.e., it denotes the difference between the second virial coefficients of the LJ and HS fluids:

$$\Delta B_2 = B_{2,LJ} - \frac{2\pi}{3} d^3. \quad (6)$$

Both the hard sphere diameter  $d$  predicted by the Barker-Henderson theory and the residual second virial coefficient  $\Delta B_2$  are expressed in terms of rapidly converging series expansion in powers of  $T^{1/2}$ . Explicit expressions of the dependence of both quantities with respect to the temperature, and the values of the coefficients of the power expansion can be found elsewhere [12].

Other thermodynamic properties are derived from the Helmholtz free energy (Eqn. (4)):

$$U_{LJ} = -T^2 \frac{\partial}{\partial T} \left( \frac{F_{LJ}}{T} \right), \quad (7)$$

$$P_{LJ} = \rho kT + \rho^2 \frac{\partial F_{LJ}}{\partial \rho}, \quad (8)$$

$$S_{LJ} = \frac{1}{T} (U_{LJ} - F_{LJ}), \quad (9)$$

$$(C_v)_{LJ} = \frac{\partial U_{LJ}}{\partial T}. \quad (10)$$

The above expressions are used to derive the optimal parameters  $\varepsilon$  and  $\sigma$  for the Lennard-Jones potential employing

the least squares method, that is, by minimizing the following cost function:

$$D = \sum_i \left( \frac{Y_{LJ}^i(\varepsilon, \sigma) - Y_{\text{exp}}^i}{Y_{\text{exp}}^i} \right)^2. \quad (11)$$

Here  $Y_{LJ}^i = U_{LJ}, P_{LJ}, S_{LJ}, (C_v)_{LJ}$  stands for the calculated internal energy, pressure, entropy and heat capacity while  $Y_{\text{exp}}^i$  denotes the corresponding experimental values.

The application of this procedure, at normal conditions of pressure and temperature (corresponding to a liquid density  $\rho_0 = 703 \text{ kg}\cdot\text{m}^{-3}$ ), yields  $\varepsilon = 230 \text{ cm}^{-1}$  and  $\sigma = 3.4 \text{ \AA}$ . These optimized parameters are used to evaluate the thermodynamic properties of liquid n-octane via CMD simulations. The cubic simulation cell contained 864 LJ particles resembling the molecules of n-octane, and its volume was adjusted to match the prescribed density. Different values of density and temperature were considered, within the limits corresponding to liquid-solid and liquid-vapour transitions of n-octane. The simulations were performed in the canonical ensemble (NVT). For simplicity, the particles were initially placed according to the points in a f.c.c. lattice, though the characteristic order of the crystalline phase was found to disappear after relatively few iterations. The initial velocities of the particles were assigned randomly, following a Boltzmann distribution and enforcing the total linear and angular momenta of the system to vanish. To reduce the calculation time, both a cut-off radius ( $r_c = 5\sigma$ ) and a neighbor list (comprising all particles within a sphere of radius  $7\sigma$  centred at the target particle) were introduced. The forces were computed according to the minimum image convention. Periodic boundary conditions were imposed along the three spatial directions. The equilibration of the system at the desired temperature (illustrated in Figure 1) typically required  $\sim 10^4$  iterations. Once the average kinetic energy of the system was stabilized, the root mean square of this quantity amounts to 3% of its value, in agreement with the theoretical prediction for the average amplitude of fluctuations corresponding to the size of the system.

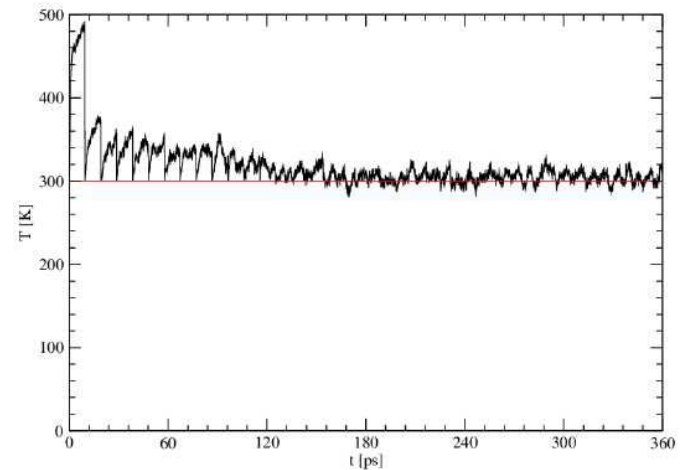


Figure 1. Time evolution of the instantaneous temperature during the equilibration phase.

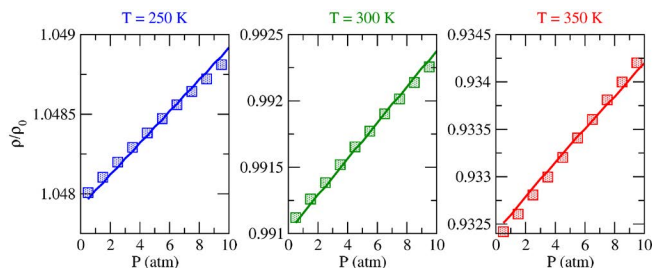


Figure 2. Pressure ( $P$ ) dependence of the dimensionless density  $\rho/\rho_0$  of the liquid, for different temperatures  $T = 250\text{K}$ ,  $300\text{K}$ ,  $350\text{K}$ . The solid curves represent the results obtained via CMD simulations, whereas the experimental points are indicated by the square markers. The characteristic density  $\rho_0 = 703 \text{ kg}\cdot\text{m}^{-3}$  is taken to be that of n-octane at standard ambient temperature and pressure.

The classical equations of motion for the LJ particles were integrated using the velocity-Verlet algorithm [1]. A time step  $\Delta t = 1 \text{ fs}$  was used as the interval between successive updates of the dynamical state of the system.

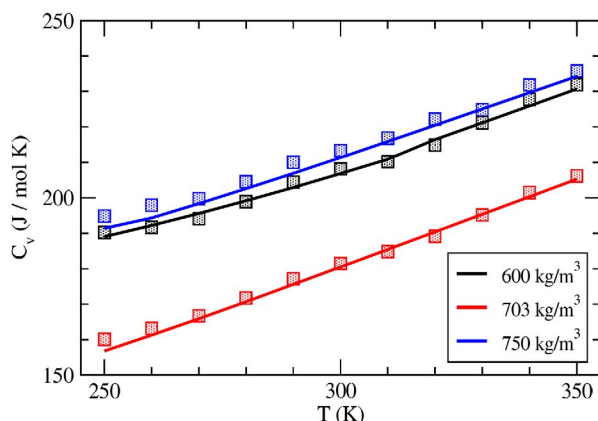


Figure 3. Temperature dependence of the heat capacity  $C_v$  at different densities  $\rho = 600 \text{ kg}\cdot\text{m}^{-3}$ ,  $703 \text{ kg}\cdot\text{m}^{-3}$ ,  $750 \text{ kg}\cdot\text{m}^{-3}$ . The solid curves represent the results of CMD simulations, whereas the corresponding experimental data points are indicated by the square markers.

Observables were computed as time averages (over  $\sim 100 \text{ ps}$ ) in the equilibrium state. For example, the pressure  $P$  and the heat capacity  $C_v$  are given by

$$PV = Nk_B T + \frac{1}{3} \left\langle \sum_{i=1}^N r_i F_i \right\rangle, \quad (12)$$

$$\langle T^2 \rangle - \langle T \rangle^2 = \frac{3}{2} NT^2 \left( 1 - \frac{3Nk_B}{2C_v} \right). \quad (13)$$

In Figure 2, the dependence of the pressure on the density of the system is shown, for different temperatures in the neighborhood of room temperature. At low pressures ( $P \leq 15 \text{ atm}$ ), the liquid state can be regarded to exist between the melting point ( $216.35\text{K}$ ) and the normal boiling point ( $398.77\text{K}$ ). Thus, the three selected values ( $T = 250\text{K}$ ,  $300\text{K}$ ,  $350\text{K}$ ) reasonably span the temperatures range of liquid n-octane. It can be seen, that the isotherms  $\rho(P, T)$  of n-octane are rather linear for these thermodynamic conditions. Such linear behavior can be anticipated from the small values of the packing fraction ( $\eta \sim 0.1-0.2$ ) for the effective hard

spheres resembling the liquid. The dependence  $\rho(P, T)$  plotted in Figure 2 agrees with the empirical equation of state of n-octane [13].

On the other hand, the temperature dependence of the heat capacity is shown in Figure 3. Again, the values obtained from the CMD simulations, carried out with the optimized interaction potential parameters, reproduce the experimental data reported for this liquid [13]. The variations of the heat capacity with respect to the density reflect the shape of the intermolecular potential well (at the density  $\rho_0 = 703 \text{ kg}\cdot\text{m}^{-3}$ , the average interparticle separation approaches the equilibrium distance,  $r_c = 2^{1/6}\sigma$ , of the effective Lennard-Jones potential).

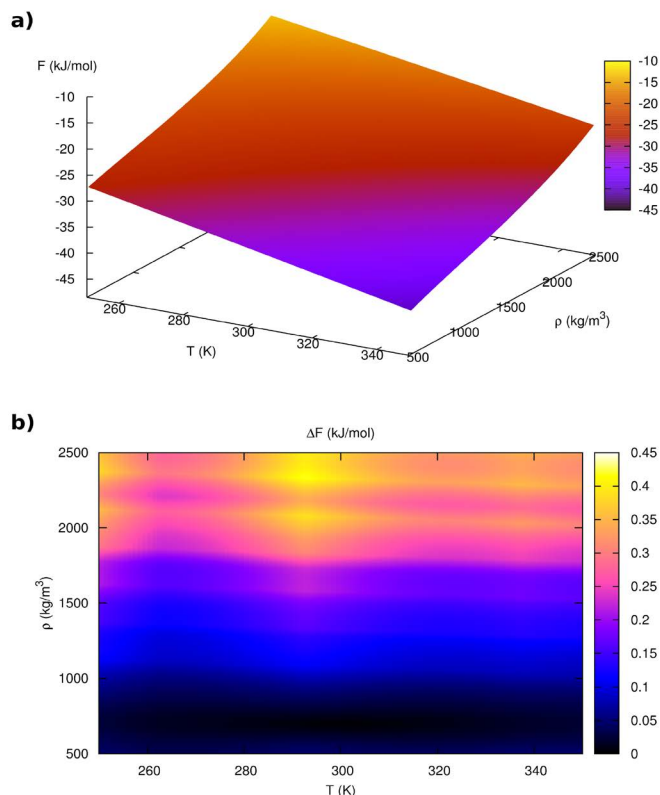


Figure 4. a) Helmholtz free energy,  $F_{LJ}$ , as a function of density  $\rho$  and temperature  $T$ , as obtained from the CMD simulations of the effective LJ fluid. b) Absolute difference  $\Delta F = |F_{LJ} - F_{\text{exp}}|$  between the simulated and the experimental values of the free energy.

The free energy (per particle) in the fluid is represented in Figure 4. It becomes apparent, that the results of the CMD simulations can be used to construct an accurate free energy functional  $F(P, T)$ . Indeed, the deviations of the calculated values of the Helmholtz free energy,  $F_{LJ}$ , with respect to the corresponding empirical data [13] is always lower than  $0.5 \text{ kJ}\cdot\text{mol}^{-1}$ . The detailed knowledge of the temperature- and pressure-dependence of the free energy would allow a continuous treatment of the solvent effects of liquid n-octane, based in distribution function theories such as the Density Functional Theory. The latter would be a more efficient approach to the modelling of dynamical processes taking place in this medium and involving a large number of particles, as it would be the case of time-resolved spectroscopy experiments.

In this work, we have applied the CMD method to the study of the thermodynamic properties of liquid n-octane, subject to a wide range of conditions of pressure and temperature. The methodology introduced here is based in the Barker-Henderson perturbation theory for a Lennard-Jones fluid. The values obtained for pressure and the heat capacity, are in correspondence with the measurements reported for this system. As an outlook, we plan to incorporate progressively the most important molecular degrees of freedom (rotational, vibrational) to determine a priori the physical properties of liquid n-octane, and to analyze the spectroscopy properties of organic molecules embedded in this medium.

- 
- [1] M. P. Allen, D. J. Tildesley, *Computer Simulation of Liquids*, (Oxford University Press, 1991)  
[2] J. M. Polson, D. Frenkel, *J. Chem. Phys.* **111**, 1501 (1999)  
[3] K. Coutinho, M. J. De Oliveira, S. Canuto, *Int. J. Quantum*

- Chem. Symp.* **65**, 885 (1997)  
[4] K. Coutinho, S. Canuto, M. C. Zerner, *Int. J. Quantum Chem.* **66**, 249 (1998)  
[5] A. Lopez Rodriguez, C. Vega, J. J. Freire, *J. Chem. Phys.* **111**, 438 (1999)  
[6] J. R. Errington, A. Z. Panagiotopoulos, *J. Chem. Phys.* **111**, 9731 (1999)  
[7] J. Cui, J. R. Elliot Jr., *J. Chem. Phys.* **116**, 8625 (2002)  
[8] J. Chang, S. I. Sandler, *J. Chem. Phys.* **121**, 7474 (2004)  
[9] J. S. de Klerk, A. Szemik-Hojniak, F. Ariese, C. Gooijer, *J. Phys. Chem. A* **111**, 5828 (2007)  
[10] J. P. Hansen, I. R. McDonald, *Theory of simple liquids*, (Academic Press, 1986)  
[11] B.-J. Zhang, *Fluid Phase Equil.* **154**, 1 (1999)  
[12] J. Kolafa, I. Nezbeda, *Fluid Phase Equil.* **100**, 1 (1994)  
[13] E. W. Lemmon, M. O. McLinden, D. G. Friend, "Thermophysical Properties of Fluid Systems" in NIST Chemistry WebBook, NIST Standard Reference Database Number 69, Eds. P.J. Linstrom and W.G. Mallard, National Institute of Standards and Technology, Gaithersburg MD, 20899, <http://webbook.nist.gov>